An ordered pathway for the assembly of fungal ESCRT-containing ambient pH signalling complexes at the plasma membrane

Antonio Galindo[1], Ana María Calcagno-Pizarelli[2], Herbert N. Arst, Jr[2] and Miguel Ángel Peñalva[1,*]

[1]Department of Molecular Medicine, Centro de Investigaciones Biológicas CSIC, Ramiro de Maeztu 9, Madrid 28040, Spain
[2]Section of Microbiology, Imperial College, Flowers Building, Armstrong Road, London SW7 2AZ, UK
*Author for correspondence (penalva@cib.csic.es)

Accepted 5 December 2011
Journal of Cell Science 125, 1784–1795

doi: 10.1242/jcs.098897

Summary

The fungal *pal/RIM* signalling pathway, which regulates gene expression in response to environmental pH involves, in addition to dedicated proteins, several components of ESCRT complexes, which suggested that pH signalling proteins assemble on endosomal platforms. In *Aspergillus nidulans*, dedicated Pal proteins include the plasma membrane receptor PalH and its coupled arrestin, PalF, which becomes ubiquitylated in alkaline pH conditions, and three potentially endosomal ESCRT-III associates, including Vps32 interactors PalA and PalC and Vps24 interactor calpain-like PalB. We studied the subcellular locations at which signalling takes place after activating the pathway by shifting ambient pH to alkalinity. Rather than localising to endosomes, Vps32 interactors PalA and PalC transiently colocalise at alkaline-pH-induced cortical structures in a PalH-, Vps23- and Vps32-dependent but Vps27-independent manner. These cortical structures are much more stable when Vps4 is deficient, indicating that their half-life depends on ESCRT-III disassembly. Pull-down studies revealed that Vps23 interacts strongly with PalF, but co-immunoprecipitates exclusively with ubiquitylated PalF forms from extracts. We demonstrate that Vps23–GFP, expressed at physiological levels, is also recruited to cortical structures, very conspicuous in *vps27Δ* cells in which the prominent signal of Vps23–GFP on endosomes is eliminated, in a PalF- and alkaline pH-dependent manner. Dual-channel epifluorescence microscopy showed that PalC arrives at cortical complexes before PalA. As PalC recruitment is PalA independent and PalA recruitment is PalC dependent but PalB independent, these data complete the participation order of Pal proteins in the pathway and strongly support a model in which pH signalling takes place in ESCRT-containing, plasma-membrane-associated, rather than endosome-associated, complexes.

Key words: Arrestin, Seven transmembrane receptor, Multivesicular body pathway, Signal transduction, *Aspergillus nidulans*

Introduction

Underlying the ability of many fungi to thrive over a broad range of pH is the existence of a transcriptional regulatory system ensuring that the synthesis of molecules mediating adaptation of cells to acidic or alkaline pH is tailored to the needs imposed by the environment. This mechanism has been most extensively studied in *Aspergillus nidulans* and *Saccharomyces cerevisiae* (Peñalva et al., 2008; Peñalva and Arst, 2004), but the robust phenotypes resulting from inactivation of this regulatory system and the larger multinucleated cells in *A. nidulans* make it ideally suited for studies correlating gene function with subcellular localisation of the cognate gene products.

The key player in this ambient-pH-mediated regulatory system is the zinc-finger transcription factor PacC. In *A. nidulans* PacC undergoes two-step proteolytic processing activation in response to alkaline ambient pH (Díez et al., 2002; Espeso et al., 2000; Hervás-Aguilar et al., 2007; Orejas et al., 1995), but only the first of these sequential proteolytic steps, known as signalling proteolysis, is regulated by ambient pH. Current evidence indicates that the signalling protease is the calpain-like PalB, which directly interacts with endosomal sorting complex required for transport (ESCRT)-III (Peñas et al., 2007; Rodríguez-Galán et al., 2009). However, it is not known how and where PalB is activated by extracellular alkaline ambient pH.

In addition to PalB, five dedicated proteins form the Pal signalling pathway mediating PacC activation. Three appear to be components of an alkaline-pH-sensing module in the plasma membrane: the helper transmembrane protein PalI, the seven-transmembrane (7-TMD) receptor PalH and the PalH-coupled arrestin-like protein PalF (Calcagno-Pizarelli et al., 2007; Herranz et al., 2005; Hervás-Aguilar et al., 2010a). Similar to mammalian β-arrestins, PalF is ubiquitylated in a receptor (PalH)- and signal (alkaline pH)-dependent manner (Herranz et al., 2005; Lefkowitz and Shenoy, 2005) and indeed ubiquitylation of arrestin-like PalF leads to constitutive signalling and PacC processing, bypassing the need for the PalH receptor (Hervás-Aguilar et al., 2010a). The remaining two proteins, PalA and PalC have been shown to interact with Vps32, the main component of ESCRT-III (Galindo et al., 2007; Vincent et al., 2003). PalA additionally interacts with YPx[L/I] motifs in PacC and thus appears to mediate recruitment of the transcription factor to the pH signalling machinery (Vincent et al., 2003; Xu and Mitchell, 2001).

Journal of Cell Science

In agreement with the known interactions of PalA, PalB and PalC, work in *S. cerevisiae* established that ESCRT-I, ESCRT-II and two ESCRT-III components, Vps20 and Vps32, are required for pH signalling (Xu et al., 2004). These findings supported the hypothesis that pH signalling would be mediated by a specialised class of ESCRT- and Pal-containing complexes assembled on the surface of endosomes, perhaps connected to the plasma membrane sensor module by endocytic trafficking (Peñalva et al., 2008), in agreement with the fact that mammalian β-arrestin ubiquitylation promotes the endocytic internalisation of arrestin-receptor complexes (Lefkowitz and Shenoy, 2005).

However, evidence argues against endocytosis and endosomal ESCRT complexes playing a role in pH signalling, because: (1) both in *S. cerevisiae* (Xu et al., 2004) and in *A. nidulans* (Calcagno-Pizarelli et al., 2011) the key ESCRT-0 component Vps27 linking multivesicular body biogenesis to phosphatidylinositol 3-phosphate (PtdIns3*P*)-containing endosomes (PtdIns3*P* is a landmark of multivesicular endosomes) is fully dispensable for signalling, and indeed PacC processing is unaffected in *rabB* deletion (*rabBΔ*) mutants unable to recruit the PtdIns3-kinase Vps34 to endosomes (Abenza et al., 2010; Calcagno-Pizarelli et al., 2011); (2) in vivo, alkaline pH drives the Vps32 interactor PalC to plasma-membrane-associated structures rather than to endosomes (Galindo et al., 2007); (3) artificial ubiquitylation of arrestin-like PalF leads to receptor-independent signalling and promotes recruitment of PalC to these cortical structures under acidic (non-signalling) conditions; (4) PalF promotes the plasma membrane, rather than endosomal, localisation of the PalH receptor (Hervás-Aguilar et al., 2010a). The finding that the *S. cerevisiae* PalF orthologue Rim8p interacts with Vps23p (Herrador et al., 2009) explained the conundrum posed by the crucial involvement of ESCRT-I, -II and -III in pH signalling and yet the complete dispensability of Vps27, suggesting a model in which receptor-activated arrestin-like PalF (Rim8p in *S. cerevisiae*) recruits Vps23 (ESCRT-I), thus priming the recruitment of ESCRT-II and -III to pH signalling complexes (Herrador et al., 2009; Hervás-Aguilar et al., 2010a). PalC recruitment to cortical structures (Galindo et al., 2007) and the finding that overexpression of Rim8p relocalises overexpressed Vps23p to the plasma membrane (Herrador et al., 2009) lend credence to the possibility that pH signalling occurs in a class of specialised ESCRT-containing complexes associated with the plasma membrane. This possibility would gain strong credibility if, for example, Vps23 expressed at physiological levels were shown to be recruited to the plasma membrane at alkaline pH.

The severely debilitating phenotype of *A. nidulans* null mutations previously precluded investigation of ESCRT in pH signalling in this organism. However, the recent finding (Calcagno-Pizarelli et al., 2011) that vigorous growth of null ESCRT strains can be rescued by mutations in the *sltA* regulatory gene, which by themselves do not affect pH signalling, allowed examination of the localisation of fluorescently tagged reporters, expressed at physiological levels, in wild-type and deficient ESCRT and *pal* (i.e. pH signalling) backgrounds. Our results provide strong evidence for a model in which PalF-dependent recruitment of Vps23 to the plasma membrane and the subsequent formation of ESCRT-containing cortical complexes enable the ordered recruitment of downstream pH signalling proteins at these locations to ultimately mediate activation of ESCRT-associated calpain-like PalB. Thus in these pH signalling complexes ESCRT-III would play signal transduction roles without facilitating membrane scission.

Results

Vps32 and Vps23 are essential and Vps27 is dispensable for the ambient pH-dependent cortical localisation of PalC

Because pH signalling is independent of Vps27, current models assume that Vps23 plays the ESCRT-recruiting role in pH signalling complexes that Vps27 plays in the multivesicular body pathway, and Vps32 acts as a scaffold for these signalling complexes. We examined the involvement of ESCRT proteins in the alkaline-ambient-pH-dependent recruitment of PalC–GFP to cortical structures. Although cells carrying single *sltA*$^{-}$ mutations, used to rescue the severely debilitating ESCRT-null mutant phenotype, behaved in the same manner as the wild-type, the additional presence of *vps23*Δ or *vps32*Δ virtually abolished PalC recruitment (Fig. 1A,C). By contrast, *vps27*Δ did not. Western blots (Fig. 1B) ruled out the possibility that the sharp decrease in PalC–GFP cortical structures resulting from *vps23*Δ or *vps32*Δ reflects increased turnover of the fluorescent protein. Thus cortical structures to which PalC is recruited meet the requirements for bona fide pH signalling complexes.

PalA is recruited to PalC cortical structures in a PalH- and alkaline-pH-dependent manner

To determine whether the second Vps32 interactor PalA is also recruited to these cortical structures we constructed a gene-replaced strain expressing physiological levels of PalA–GFP. Under acidic conditions, PalA localises to the cytosol, to a few motile cytosolic structures (almost certainly early endosomes) and to the spindle pole bodies (SPBs) (supplementary material Fig. S1; SPB localisation will be addressed elsewhere). Upon shifting cells to alkaline conditions, PalA–GFP was clearly recruited to cortical structures resembling those seen with PalC (Fig. 1D–F). As for PalC, PalA recruitment was dependent on the 7-TMD receptor PalH (Fig. 1F, Fig. 2E). Fig. 2A shows that, in cells expressing physiological levels of fluorescently tagged PalA and PalC from gene-replaced alleles, PalA–mCherry and PalC–GFP colocalise in the same alkaline-pH-induced cortical structures, strongly indicating that activation of the pH signal transduction pathway involves the recruitment of both PalC and PalA to plasma-membrane-associated signalling complexes. Anti-GFP western blots showed that the physiological levels of PalA and PalC are very similar (Fig. 2C), as are the fluorescence levels of cortical pH signalling foci, irrespective of whether they are labelled with PalA– or PalC–GFP (data not shown).

PalA recruitment to cortical foci is Vps32 and PalC dependent but PalB independent

PalA, like PalC, is a Vps32 interactor (Vincent et al., 2003; Xu and Mitchell, 2001). Thus we addressed whether PalA cortical recruitment also involves this ESCRT-III principal component. Alkaline pH shift experiments demonstrated that PalA cortical foci were essentially absent in *vps32*Δ cells (Fig. 2B), despite the fact that neither of the mutant backgrounds used (*sltA54* or *sltA54 vps32*Δ) affected the steady-state levels of PalA–GFP (Fig. 2C). The dependence of PalA and PalC cortical recruitment on Vps32 strongly implicates Vps32 in the formation of the plasma-membrane-associated signalling complexes.

PalC–GFP recruitment is dependent on PalF and independent of PalA (Galindo et al., 2007; Hervás-Aguilar et al., 2010a). By contrast, PalA recruitment is fully dependent on PalC (Fig. 2D,E, *palC*Δ) and independent of PalB [Fig. 2D,E,

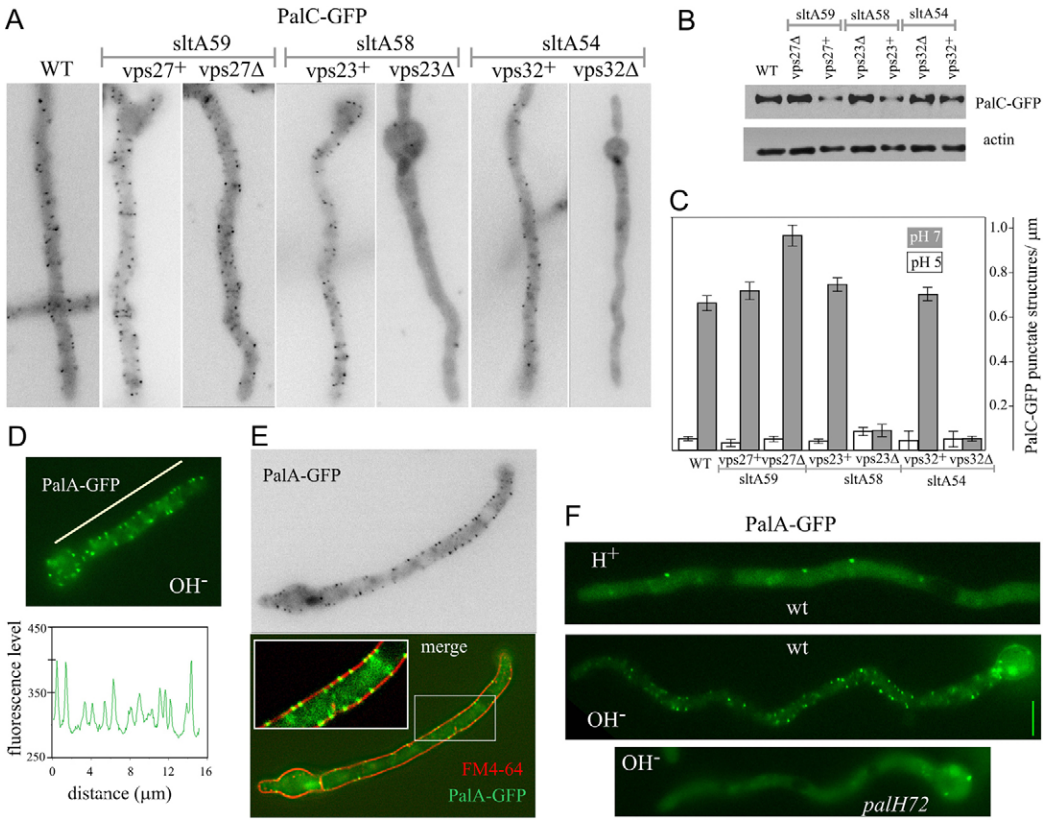

Fig. 1. ESCRT dependence of PalC–GFP recruitment to cortical structures. PalA also relocalises to cortical structures in a pH signalling-dependent manner. (**A**) Localisation of PalC–GFP to cortical structures upon shifting cells of the indicated genotypes to alkaline pH. Controls are strains carrying the different *sltA*$^{-}$ single mutations used to rescue the severely debilitating null ESCRT mutations. (**B**) Western blot analysis showing that null ESCRT mutations do not result in reduced levels of PalC–GFP. Anti-actin was used to monitor loading. (**C**) The average number of cortical PalC–GFP-containing structures per unit length in at least 25 hyphae for each of the indicated genotypes. Bars indicate the standard errors. (**D**) Cortical structures containing PalA–GFP expressed at physiological levels in a germling shifted from acidic to alkaline conditions. A linescan (length indicated by white bar) along the cortex is shown below. (**E**) PalA–GFP-containing structures overlap with the plasma membrane labelled with the lipophilic dye FM4-64 (red). (**F**) Recruitment of PalA–GFP to cortical structures is PalH dependent. Wild-type and *palH72* (a null *palH* allele) cells were shifted from acidic to alkaline conditions (only alkaline conditions shown for *palH72*). Scale bar: 5 µm.

palB38 is a classical *palB* null allele (Peñas et al., 2007)]. These key data show that PalC acts downstream of PalF and upstream of PalA and that PalA acts upstream of the calpain-like PalB, thus establishing the order of action of Pal proteins (see Discussion).

Transient ambient-pH-dependent recruitment of PalC and PalA to cortical foci

Previous work (Galindo et al., 2007) suggested that PalC recruitment to cortical structures is transient. To analyse this transient recruitment, we cultured hyphae expressing PalC–GFP under acidic (pH 5) conditions in a microscopy chamber and shifted them to alkaline conditions (pH 7.2) before starting to acquire time-lapse sequences in the GFP channel (supplementary material Movies 1 and 2). PalC–GFP at these cortical structures appeared as recurring fluorescent dots (Fig. 3A,C). These dots, unlike endocytic sites labelled with AbpA^{Abp1} (Araujo-Bazán et al., 2008), are essentially static. Therefore, the arrival and departure of PalC at these structures could be tracked with montages made of individual frames (Fig. 3C) or with kymographs, in which PalC–GFP gave rise to discontinuous lines perpendicular to the distance scale. The length of these lines reflects the time of residence of PalC–GFP (the only source of PalC) in the structures (Fig. 3A, kymograph horizontal lines), which was determined to be ~36 seconds (n=50 structures). PalA–GFP-containing cortical structures also appeared as recurring foci (supplementary material Movie 3; Fig. 3B,D), leading to short lines in kymographs (Fig. 3B). The half-life of 'alkaline' PalA–GFP foci (~68 seconds; n=50) was longer than that of PalC–GFP foci. For either PalC–GFP or PalA–GFP foci, fluorescence recurrently 'oscillated' at the same cortical locations (Fig. 3A–D), suggesting the existence of specialised signalling domains in the plasma membrane. Thus, all the above experiments strongly suggest that activation of the ambient pH signalling pathway results in the formation of membrane-associated complexes transiently containing the Bro1 domain protein PalA and the Bro1-domain-like protein PalC.

PalC precedes PalA in arrival at and departure from cortical structures

We next used a strain co-expressing (at physiological levels) PalC–GFP with PalA–mCherry to acquire dual-channel time series of cells shifted to alkaline conditions 'on the stage'. The time resolution achieved was 4.4 frames/second. Frame-by-frame

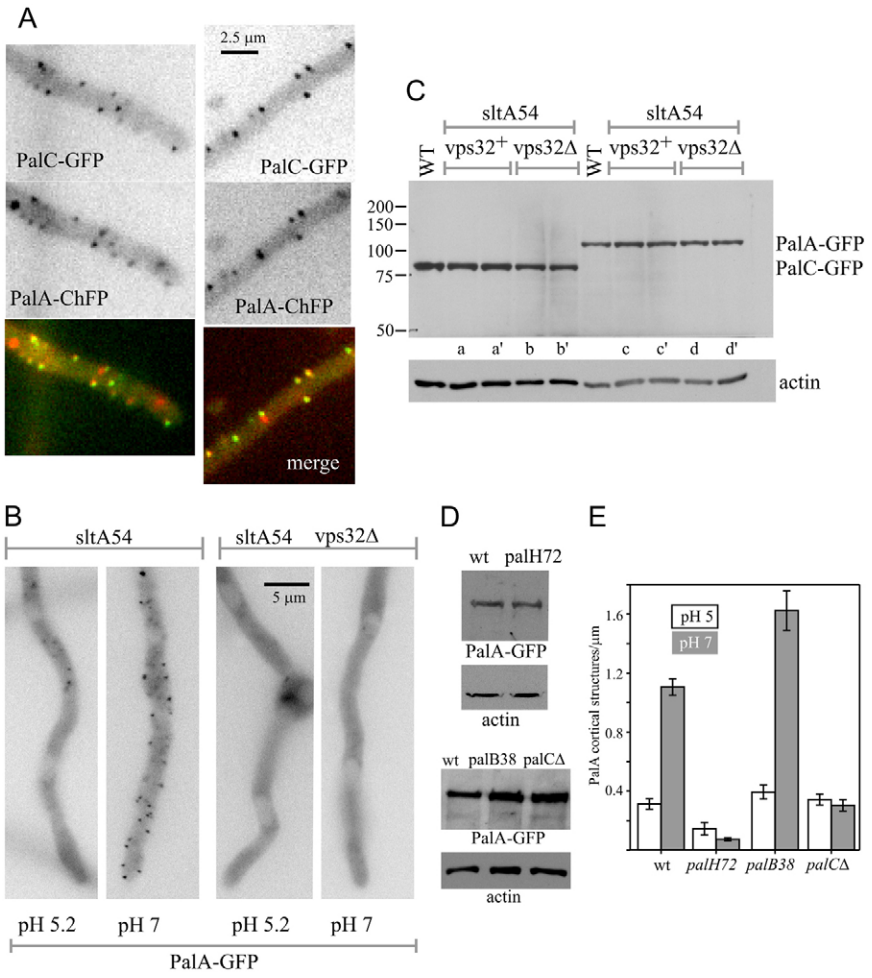

Fig. 2. Alkaline-pH-driven localisation of PalA to cortical structures is dependent on Vps32, PalH and PalC. (**A**) Colocalisation of PalA–mCherry and PalC–GFP expressed at physiological levels. (**B**) PalA–GFP localisation to cortical structures is Vps32 dependent. (**C**) Anti-GFP western blot demonstrating that the lack of cortical PalA localisation in the *vps32*Δ background is not due to decreased levels of PalA–GFP. PalA–GFP and PalC–GFP show similar steady state levels (anti-actin was used to monitor loading). Two independent clones are shown for each genotype (a, a′, etc.). (**D**) As in C for PalA–GFP in null *palH* (*palH72*), null *palB* (*palB38*) and *palC*Δ backgrounds. (**E**) The numbers of punctate structures per unit length in at least 25 hyphae for each of the indicated mutant conditions.

visual inspection of single foci showed that PalC precedes PalA in its arrival at and departure from these structures (supplementary material Movie 4, and Fig. 3E, lower panel, showing one example as a dual channel composition). This was confirmed by determining average signals in the corresponding GFP and mCherry frames. For any given structure these values were normalised to the frame showing the maximal signal in each channel (i.e. the 'peak' intensity for each channel). These relative intensity values were plotted versus time. To allow comparison between different series and/or structures, the time point immediately preceding that at which the PalA (mCherry) signal for any given structure was increased over background was arbitrarily chosen as the zero time point. The plots illustrating the individual data showed that the initiation of GFP fluorescence clearly preceded that of mCherry fluorescence (supplementary material Fig. S2 shows primary data for six structures). The conclusion that PalC precedes PalA in arrival at the pH signalling structures was further reinforced after averaging data for 50 structures (Fig. 3E). This conclusion agrees with the above finding that PalA localisation is dependent on PalC but independent of PalB.

Vps4 downregulation dramatically increases the time of residence of PalC–GFP at cortical pH signalling sites

ESCRT-III forms a complex on membranes that is disassembled by Vps4 (Teis et al., 2008). The complete dependence that pH signalling complexes have on the major ESCRT-III component Vps32 is consistent with a mechanism in which plasma-membrane-associated foci containing ESCRT-III polymers mediate recruitment of the Vps32 interactors PalA and PalC. If so, reduced levels of the Vps4 ATPase would be expected to increase the time of residence of PalC and PalA in the foci. To test this prediction, we replaced the resident gene encoding Vps4 with two regulatable expression alleles of Vps4, using the nitrite reductase promoter $niiA^{p}$ (Hervás-Aguilar and Peñalva, 2010), which is nitrate-inducible and ammonium repressible. These two alleles, denoted *vps4-1* and *vps4-ha3*, drive expression of wild-type Vps4 and (HA)3-Vps4, respectively (Fig. 4). They are the only source of Vps4 in strains carrying them.

ESCRT gene deletions cause a severely debilitating phenotype (Calcagno-Pizarelli et al., 2011). Thus, Vps4 downregulation was expected to impair growth markedly. Indeed *vps4-1* strains grew very poorly on ammonium, indicating that, under such conditions, Vps4 levels are limiting (Fig. 4A). By contrast, *vps4-1* strains grew as well as the wild type on urea, a 'neutral' (i.e. non-inducing and non-repressing) nitrogen source that results in basal levels of expression of *niiA* (Fig. 4A). Unlike urea, full induction of *vps4-1*, with nitrate, impaired growth (Fig. 4A). Therefore, these data strongly suggest that in *vps4-1* cells the downregulated levels of Vps4 on ammonium are insufficient to support growth, whereas those on nitrate are excessively high, leading to toxicity. Western blot analysis of

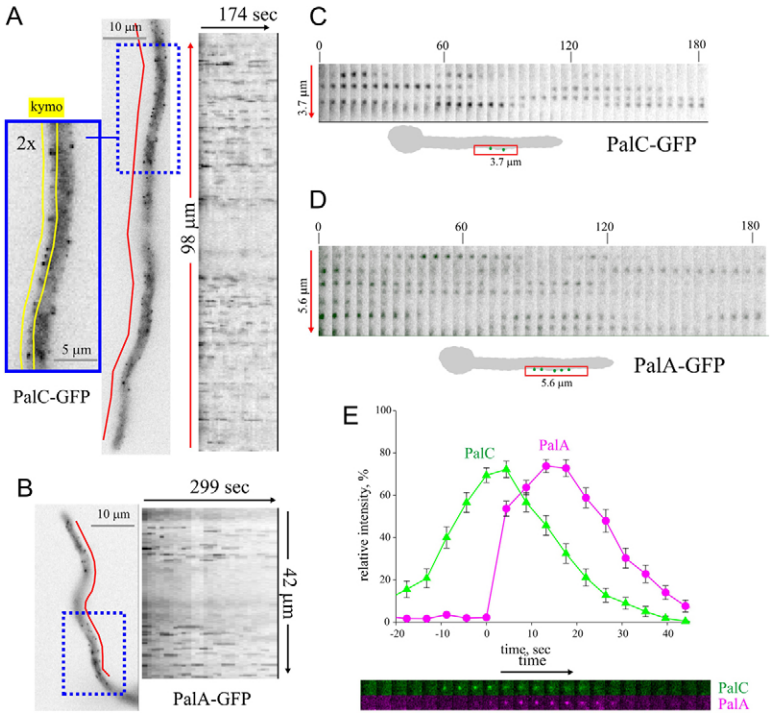

Fig. 3. Transient residence of PalC and PalA in pH signalling structures. (**A**) Kymograph analysis of a time-lapse acquisition series of a hypha expressing PalC–GFP that had been shifted to alkaline conditions. The red line in the middle panel represents the length dimension of the kymograph. The left panel is shown at double the magnification to indicate the location relative to the cell of the cortical region used for the kymograph, such that any cytosolic fluorescence signal was avoided. (**B**) As above for a hypha expressing PalA–GFP. (**C**) Montage of individual frames of a PalC–GFP time-lapse sequence, using the region indicated in the cartoon. (**D**) As C, for PalA–GFP. (**E**) The relative intensities of 50 cortical structures containing PalA–mCherry and PalC–GFP expressed at physiological levels were plotted against time, arbitrarily setting the 0 time point to the point preceding the first time point at which the PalA–mCherry signal increased above background for any given structure. Bars indicate the standard errors.

vps4-1 cells using a polyclonal anti-Vps4 antiserum (Fig. 4B) demonstrated that in cells cultured on ammonium Vps4 was virtually undetectable, whereas on nitrate the level was markedly higher than in the wild type. On urea, levels were detectable but below wild-type levels, indicating that Vps4 is normally in excess, as urea levels suffice for virtually normal growth.

vps4-ha3 mutants did not grow on ammonium either (Fig. 4A). However, *vps4-ha3* strains, unlike *vps4-1* strains, showed impaired growth on urea, strongly indicating that attachment of (HA)3 to the N-terminal MIT domain reduces Vps4 function. To confirm this and to monitor the extent of (HA)3-Vps4 downregulation achieved with *vps4-ha3*, relative to the physiological levels, we constructed a transgene driving (HA)3-Vps4 expression under the control of $vps4^{p}$. In single copy, this $vps4^{p}$::(HA)3-Vps4 transgene does not complement the *vps4-1* growth defect on ammonium, indicating that (HA)3-Vps4 is hypofunctional (data not shown). Anti-HA western blots showed that, as for untagged Vps4, the tagged (HA)3-Vps4 urea-cultured levels obtained with $niiA^{p}$ (*vps4-ha3* allele) were lower than those attained with the physiological $vps4^{p}$ promoter (in a strain carrying the wild-type *vps4* allele, to maintain viability; Fig. 4C). The level of *vps4-ha3* in ammonium-cultured cells was barely detectable (Fig. 4C). In contrast to *vps4-1* strains, *vps4-ha3* strains grew like wild-type cells on nitrate, correlating with elevated (HA)3-Vps4 levels (Fig. 4C), strongly indicating that overexpression compensates for impaired function. In summary, *vps4-1* and *vps4-ha3* cells cultured on ammonium are markedly deficient in Vps4 function. *vps4-ha3* also behaves as a partial loss-of-function allele on urea but resembles the wild type on nitrate. By contrast, the levels of untagged Vps4 (*vps4-1*) on urea are functionally sufficient but the levels on nitrate impair growth because of overexpression toxicity.

We next addressed the effects of Vps4 downregulation in the alkaline-pH-induced recruitment of PalC–GFP to cortical foci. None of the tested conditions (i.e. levels of expression) affected the formation of PalC–GFP foci induced by alkaline pH (supplementary material Fig. S3; note that *vps4-1* spores were able to germinate and give rise to germlings on ammonium). However, kymographs from time-lapse sequences (Fig. 4D) showed that whereas recruitment was transient under Vps4-sufficient (nitrate or urea) conditions, Vps4-deficient conditions (ammonium) dramatically increased the time of residence of PalC–GFP at these structures, such that they were seen as continuous vertical lines for the complete duration of the kymographs (Fig. 4D). *vps4-ha3* cells behaved similarly to wild-type cells on nitrate (data not shown). However, both ammonium (Fig. 4D) and urea (data not shown) led to an effect similar to that caused by ammonium downregulation of wild-type Vps4. These data are strong evidence that ESCRT-III components localise to cortical sites, where they mediate the transient recruitment of PalC and PalA until disassembled by Vps4.

PacC undergoes two-step proteolytic activation. Alkaline ambient pH results in the Pal-pathway-dependent conversion of full length PacC72 to PacC53, a committed intermediate that is converted into the fully processed, functional form PacC27 by the proteasome (Fig. 5). We hypothesised that inefficient disassembly of pH signalling structures resulting from Vps4 deficiency should lead to PacC proteolytic activation under inappropriate circumstances. In *vps4-1* cells cultured on urea or nitrate, or in *vps4-ha3* cells cultured on nitrate, PacC proteolytic processing proceeded as in wild-type cells (Fig. 5). In marked contrast, in *vps4-1* cells cultured on ammonium, or in *vps4-ha3* cells cultured on urea or ammonium, conditions leading to deficient Vps4 activity, processing assays unambiguously established that PacC72 is converted into PacC53 and PacC27 in a pH-signalling-independent manner. Under acidic conditions PacC53 and PacC27 levels, normally below detection in the wild type, were high, apparently at the expense of PacC72, which was very low or even undetectable (Fig. 5, red boxes). Vps4-deficient

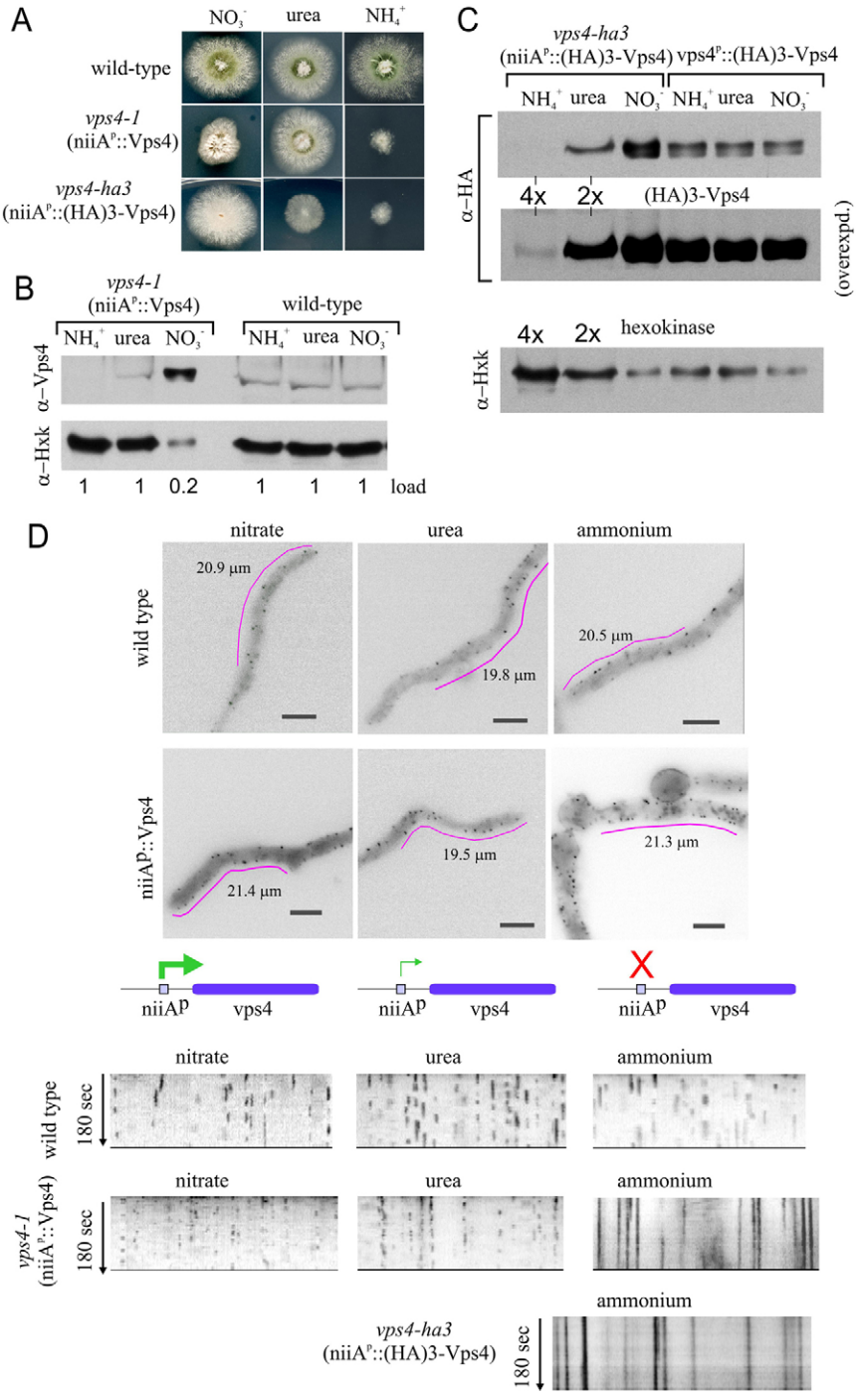

Fig. 4. Stability of PalC–GFP-containing cortical structures is dramatically increased upon Vps4 deficiency. (**A**) Growth phenotypes of the wild-type strain compared with strains expressing Vps4 (*vps4-1*) or (HA)3-Vps4 (*vps4-ha3*) under the *niiA* promoter. Minimal medium contained the indicated nitrogen sources. (**B**) Anti-Vps4 blots of wild-type and *vps4-1* cells using a polyclonal rabbit antiserum. Cells were cultured with the indicated nitrogen sources. Nitrate, urea and ammonium lead to full induction, basal levels of expression and complete repression of the *niiA* promoter, respectively. The NO_3^- *vps4-1* lane labelled '0.2' contains 1/5 of the material of the other lanes, to avoid an excessive Vps4 signal. The different nitrogen sources have no effect on Vps4 levels in the wild-type strain. Hexokinase (Hxk) was used as a loading control. (**C**) Anti-HA western blots of *vps4-ha3* cells and of cells expressing (HA)3-Vps4 under the control of the $vps4^p$ promoter, cultured with the indicated nitrogen sources, as above. Two exposures of the blot reacted with the anti-HA antibody are shown. Overexposure (bottom) allowed detection of a faint band in the ammonium-cultured *vps4-ha3* cells. Ammonium and urea lanes of the *vps4-ha3* section were overloaded four and two times, respectively, compared with the other lanes. Hexokinase was used as the loading control. (**D**) Hyphae showing the positions (magenta lines) along the cortex of the kymographs (180 seconds time-lapse sequences) shown below. For convenience, their 'distance' dimension (length indicated) corresponds here to the horizontal axis, and thus lines generated by cortical pH signalling structures are vertical; kymographs show the stability of PalC–GFP at alkaline-pH-induced cortical structures from cells cultured under the indicated conditions for Vps4. In the lower kymograph, an example of a *vps4-ha3* [$niiA^p$::(HA)3-Vps4] cell cultured under repressing conditions is shown.

conditions do not increase the number of signalling foci under acidic conditions (their abundance being alkaline-pH-dependent as in the wild type; supplementary material Fig. S3). Therefore, these results indicate that the abnormally long-lived pH signalling foci in the mutants amplify the basal levels of PacC processing to an extent that normally occurs exclusively under alkaline pH conditions.

A. nidulans Vps23 strongly interacts with arrestin-like PalF

An important question is what determines the plasma membrane recruitment of ESCRT-III. Experiments in *S. cerevisiae* pointed to Vps23 as one connection between the alkaline pH sensing module and ESCRTs (Herrador et al., 2009). Pull-down experiments using the *A. nidulans* Vps23 UEV domain strongly supported this conclusion. GST fusion proteins carrying either full length Vps23 (not shown) or the $Vps23^{UEV}$ domain (residues 1–159 of *A. nidulans* Vps23) pulled down arrestin-like PalF-(HA)3 from extracts as efficiently as a PalH cytosolic tail construct (residues 349–760 including the two arrestin-binding regions) (Herranz et al., 2005), but did not pull-down the unrelated bait Vps41 (Fig. 6A,B). PalF-(HA)3 extracts prepared after growth in acidic and alkaline (thus leading to PalF

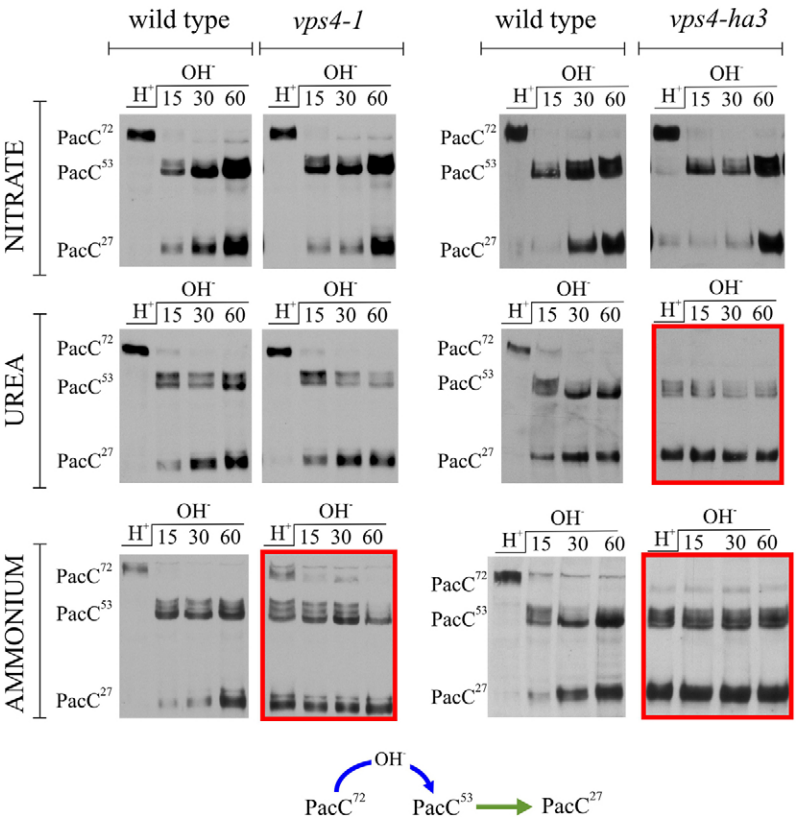

Fig. 5. Abnormal proteolytic processing activation of PacC when Vps4 is deficient. Wild-type, *vps4-1* and *vps4-ha3* cells expressing Myc-tagged PacC were cultured with the indicated nitrogen sources in acidic pH conditions and shifted to alkaline pH conditions. Samples were taken before the shift and at the indicated time points (15–60 minutes) after the shift and analysed by anti-Myc western blotting. Red boxes indicate situations in which PacC53 and PacC27 levels, normally below detection in acidic-grown wild-type cells, were high, apparently at the expense of PacC72.

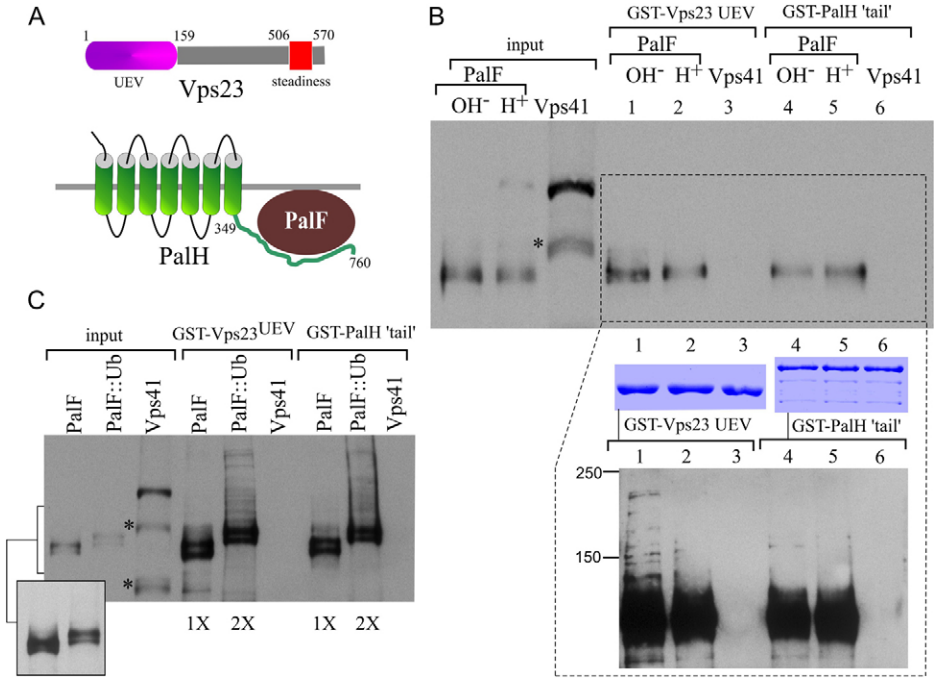

Fig. 6. Pull-down interaction between Vps23 and PalF. (**A**) Schemes of Vps23 and PalH, whose UEV domain and cytosolic tail, respectively, were used in the GST pull-down assays. (**B**) Soluble protein extracts of strains expressing PalF-(HA)3 or Vps41-(HA)3 cultured under acidic (H^+) or alkaline (OH^-) conditions were incubated in pull-down assays with glutathione–Sepharose beads loaded with GST–Vps23^{UEV} or GST–PalH 'tail' (i.e. the cytosolic tail of PalH). Material co-purifying with the baits was recovered by centrifugation, washed and analysed by anti-HA western blot. The lower panel is an overexposure of the boxed region in the upper panel, aimed at detecting the lower-mobility ubiquitylated bands of PalF. Input lanes contain 5% of the material used for pull-downs. The Coomassie-Blue-stained portion of the gel containing the baits is shown above the high exposure panel. (**C**) As B, but using PalF-(HA)3 and PalF-(HA)3–Ub extracts as preys. The inset is a longer exposure of the PalF input lanes (5% of the pulled-down material). 1 × and 2 × indicate that PalF–Ub lanes contain twice the amount of material as the PalF lanes. Asterisks indicate proteolytic products of Vps41.

ubiquitylation) conditions showed that although GST–Vps23^{UEV} pull-down material would appear to be very slightly enriched in the ubiquitylated forms of PalF, the non-ubiquitylated forms were also efficiently bound (Fig. 6B). In agreement, GST–Vps23^{UEV} pulled down a PalF–Ub protein fusion apparently as efficiently as PalF (Fig. 6C, note that PalF–Ub pull-down lanes contain twice the loading of PalF ones). Therefore these assays establish that, as in *S. cerevisiae*, *A. nidulans* Vps23 links the ESCRT machinery to the receptor–arrestin complex. However, in view of the lack of preference shown by Vps23^{UEV} for PalF–Ub, they do not satisfactorily explain the crucial role that PalF–Ub must play as alkaline ambient pH transducer [note that ubiquitin attachment to PalF leads to constitutivity (Hervás-Aguilar et al., 2010a)] (see Discussion).

Under alkaline pH conditions, Vps23 pulls down ubiquitylated PalF exclusively

The above experiments cannot discriminate differences in relative affinities, and thus their results might simply reflect that the 'basal' affinity of GST–Vps23 for PalF in vitro, almost certainly mediated by the SxP motifs of the latter (see Discussion), is sufficiently high to efficiently pull-down the arrestin, whether ubiquitylated or not. Thus we analysed, by anti-HA western blotting, anti-GFP immunoprecipitates of a PalF-(HA)3 strain also expressing, at physiological levels, Vps23–GFP (see below), using extracts from cells cultured in acidic or alkaline conditions (Fig. 7). In this strain and in the PalF-(HA)3 control (i.e. without Vps23 tagging), PalF was ubiquitylated in an alkaline-pH-dependent manner, resulting in a smear of PalF bands showing lower mobility than non-ubiquitylated PalF (Fig. 7, lanes 1, 2, 4, 5, upper panels) (Herranz et al., 2005; Hervás-Aguilar et al., 2010a). Despite the large predominance of non-ubiquitylated PalF, only ubiquitylated PalF species present in cells shifted to alkaline conditions co-immunoprecipitated with Vps23–GFP (Fig. 7, lane 7, arrow). No PalF bands were co-immunoprecipitated from extracts of acidic-grown cultures (Fig. 7, lane 6), in which PalF is not ubiquitylated, nor from extracts from acidic- or alkaline-grown cells that did not express the Vps23–GFP bait (Fig. 7, lanes 9 and 10). Thus these experiments establish that ubiquitylated PalF and Vps23–GFP occur together in alkaline-pH-induced protein complexes in vivo.

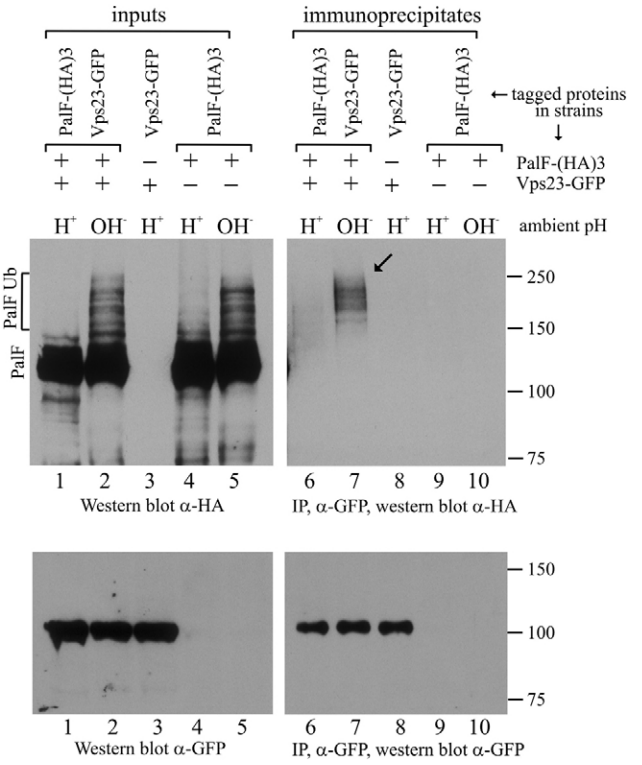

Fig. 7. Vps23–GFP immunoprecipitates contain exclusively ubiquitylated PalF species. Lysates of cells cultured under acidic or alkaline conditions and expressing the indicated tagged proteins were immunopreciptated with anti-GFP antibodies and analysed by anti-HA or anti-GFP western blotting, as indicated. For anti-HA and anti-GFP western blots input lines contained 5% and 15% of the pulled-down material, respectively. The arrow indicates ubiquitylated species of PalF.

Under alkaline conditions, Vps23–GFP localises to cortical sites in a Vps27-independent, but PalF-dependent manner

Next we studied whether the presence of ubiquitylated PalF in Vps23-containing complexes correlates with recruitment of ESCRTs to the plasma membrane. Recruitment of Vps32 to cortical structures cannot be studied in vivo because tagging with fluorescent proteins prevents its function (Hervás-Aguilar et al., 2010b; Nickerson et al., 2006). Thus, in view of the crucial role that Vps23 appears to play in pH signalling, we investigated this ESCRT-I protein. We found that strains in which the resident *vps23* gene had been replaced by the GFP-tagged version (Materials and Methods) grew normally, indicating that Vps23–GFP is functional [as Vps23 is virtually essential (Calcagno-Pizarelli et al., 2011)]. This allowed study of the localisation of Vps23 expressed at physiological levels, avoiding overexpression artefacts. In acidic conditions Vps23 localises to the cytosol and to punctate cytosolic structures that undeniably represent endosomes because many showed the characteristic movement of early endosomes (EEs) in kymographs (Fig. 8A), and because in the absence of Vps27, Vps23–GFP does not localise to them (Fig. 8B). Studies on the potential recruitment of Vps23 to cortical sites were hampered by its presence in these endosomes, which often move along microtubule tracks in the vicinity of the cortex (supplementary material Movie 5). Thus, we converted time-lapse sequences of Vps23–GFP into sum projections, which essentially flattened the signal of moving endosomes and enhanced that of static structures, allowing us to detect clearly Vps23–GFP cortical foci in cells that had been shifted to alkaline conditions (Fig. 8C). Vps23–GFP foci were rare in cells continuously cultured under acidic conditions (Fig. 8B). Indeed recruitment of Vps23–GFP to cortical foci is PalF dependent (Fig. 8C), demonstrating that it requires activation of the ambient pH-signalling pathway (Vps23–GFP levels were unaffected by *vps27*Δ, *sltA59*, *sltA59 vps27*Δ or *palF15* mutations, data not shown). The finding that such alkaline-pH-dependent recruitment was seen in *vps27*Δ cells indicated that this cortical localization is unrelated to the role that Vps23 plays in the multivesicular body pathway. Because *vps27*Δ eliminates the endosomal Vps23–GFP signal, we used these mutant cells to demonstrate unambiguously that pH-signalling-related Vps23 cortical structures clearly overlap with the plasma membrane stained with the lipophilic dye FM4-64 (Fig. 8D).

Finally we constructed a *vps27*Δ strain expressing Vps23–GFP and PalA–mCherry and acquired time-lapse sequences in the red

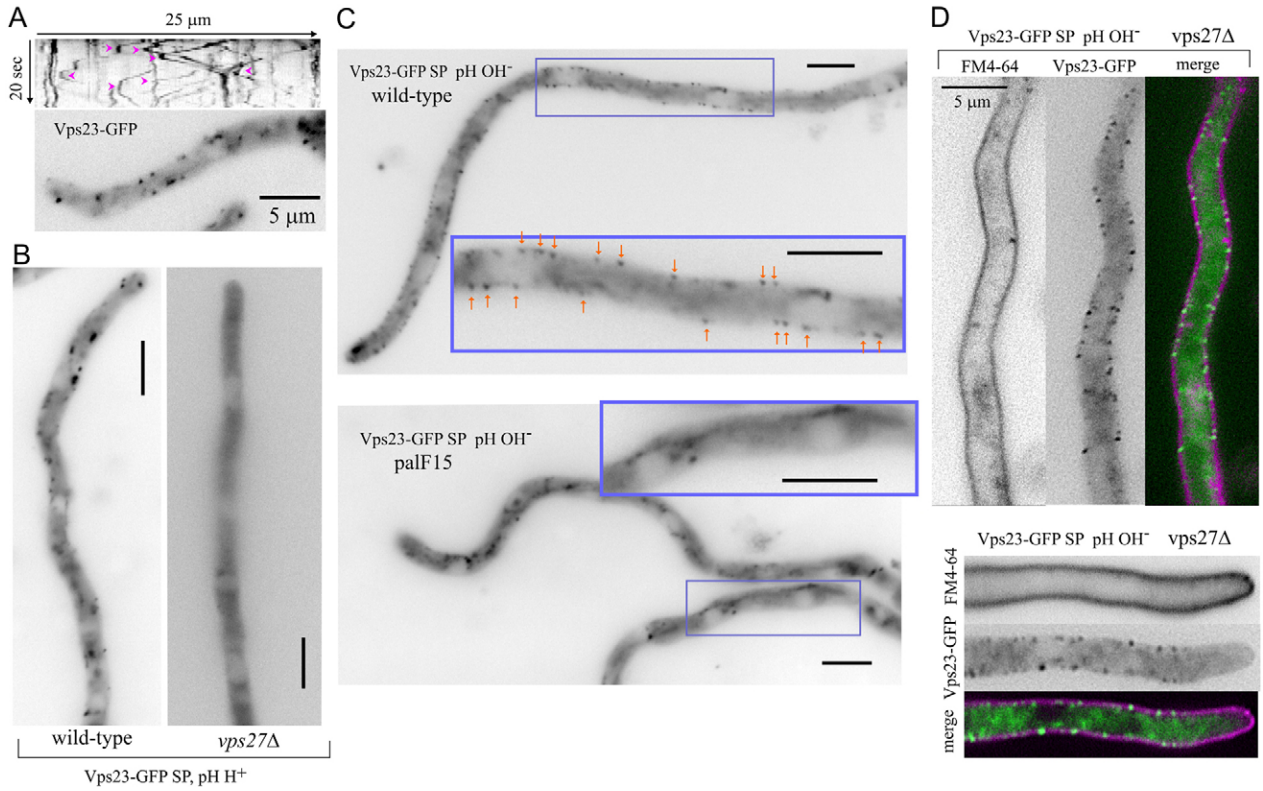

Fig. 8. Vps23–GFP localisation to endosomes and, in alkaline pH conditions, to cortical structures. (**A**) In acidic conditions, Vps23 localises to bidirectionally motile structures (early endosomes) and to static cytosolic punctate structures (late endosomes). Motile structures appear as diagonal lines in the kymograph shown on the top of the image (corresponding to supplementary material Movie 5). Magenta arrowheads indicate a change in the direction of EE movement. (**B**) In *vps27*Δ cells cultured under acidic conditions Vps23–GFP loses its endosomal localisation and becomes cytosolic. Both images are sum projections (SP) of time-lapse series. (**C**) Sum projections of time-lapse series of wild-type and null *palF15* cells shifted to alkaline pH. Cortical Vps23–GFP structures (orange arrows in the 2× magnified insert) are conspicuous in the wild type and absent in the mutant. (**D**) Cortical Vps23–GFP structures become very prominent in the absence of Vps27, which prevents the endosomal but not the alkaline pH-induced cortical Vps23–GFP localisation. The plasma membrane was stained with FM4–64 (magenta). Scale bars: 5 μm.

and green channels. The Vps23–GFP signal obtained under such conditions was very weak, precluding any dynamic analysis. Sum projections showed that Vps23–GFP-containing cortical structures were more abundant than PalA–mCherry-containing structures. However, 77% of 448 PalA-containing structures from 27 hyphae colocalised with Vps23 (supplementary material Fig. S4), clearly linking cortical Vps23–GFP-containing structures and pH signalling complexes.

Discussion

A model for the initial steps of the ambient pH-signalling pathway is shown in Fig. 9. The 7-TMD protein PalH that localises to the plasma membrane with the aid of the helper PalI (not depicted) must be the ambient pH sensor. The cytosolic PalH tail binds strongly to arrestin-like PalF and this interaction discourages trafficking of PalH away from the plasma membrane (Hervás-Aguilar et al., 2010a). In alkaline conditions PalF is ubiquitylated in a PalH-dependent manner. Ubiquitylated PalF mediates recruitment of Vps23 (Fig. 9) and perhaps of other ESCRT components (see below) to plasma membrane signalling complexes, thus linking ambient pH reception with the plasma membrane assembly of ESCRTs. Once at the plasma membrane, Vps23 promotes the recruitment of ESCRT-III components, possibly with ESCRT-II involvement, as suggested by the findings that at least ESCRT-II *vps36*Δ prevents pH signalling in *Aspergillus* and that *vps36*Δ, *vps22*Δ and *vps25*Δ prevent signalling in yeast (Calcagno-Pizarelli et al., 2011; Xu et al., 2004).

Following ESCRT-III assembly on the plasma membrane, its major component Vps32 (Teis et al., 2008) recruits, or crucially cooperates in, recruitment of one of its Pal interactors, the Bro1 domain-like PalC (Galindo et al., 2007). PalA arrives to these complexes after PalC incorporation (Fig. 3) and PalA recruitment to cortical pH signalling sites is PalC dependent. Finally, calpain-like protease PalB, which is dispensable for PalA recruitment (Fig. 2E), is itself recruited to these complexes through interaction of its MIT domain with Vps24 and possibly through additional, as yet uncharacterised interactions with Vps32 or other ESCRT components (Ito et al., 2001; Rodríguez-Galán et al., 2009). What are the different roles that Vps32 binders PalA and PalC play in these complexes, how is ESCRT-III polymerisation controlled to prevent budding events (Hurley and Hanson, 2010), and what is the stoichiometry of ESCRT and Pal proteins in these complexes, are questions for future investigation. Finally a major unanswered question is how this ordered chain of events leads to PalB protease activation. It is worth noting that Maki and coworkers have recently reported that the MIT domain-containing calpain 7 protease, the human PalB orthologue, is activated by recruitment to ESCRT components (Osako et al., 2010).

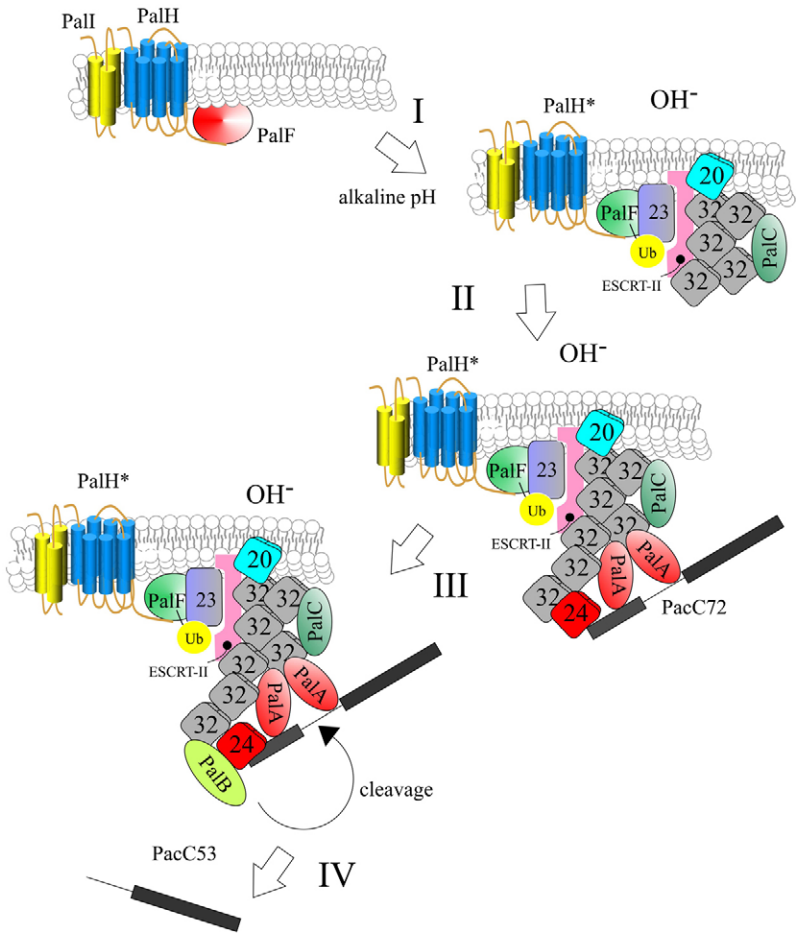

Fig. 9. Proposed model of pH signalling. (**I**) In alkaline pH conditions activated PalH (PalH*) transmits a signal across the membrane resulting in the activation of arrestin-like PalF, which becomes ubiquitylated. PalF–Ub recruits the ESCRT machinery to cortical locations in a Vps27-independent manner, in a process that involves at least Vps23 of ESCRT-I. This results in Vps32 polymerisation and PalC recruitment to the complex through interaction with Vps32. (**II**) PalA arrives at the complex; PalA recruitment is also Vps32-mediated, does not require PalB but necessitates a function provided by PalC. The arrival of PalA implies that PacC can be recruited to these sites through the two YPx[L/I] motifs flanking the signalling protease box in the transcription factor. As in endosomal ESCRTs, Vps24 would be recruited with Vps2 (not shown) to arrest Vps32 polymerisation. (**III**) PalB is recruited to these sites in a process involving Vps24 and other, as yet unidentified, partners. (**IV**) PalB cleaves PacC72 within the signalling protease box to yield PacC53.

In this speculative model the molecular details of the intracellular switch(-es) triggering this cascade are insufficiently understood. It is clear that Vps23 plays an important role in association with PalF, as shown by the strong binding detected between *A. nidulans* Vps23 and PalF (Fig. 6) and between *S. cerevisiae* Vps23p and Rim8p (Herrador et al., 2009), and also by the inability of PalF null mutants to recruit Vps23–GFP to cortical sites (Fig. 8C). Also well established is the key role that PalF ubiquitylation must play, as expression of PalF–Ub at physiological levels results in constitutive PacC processing and recruitment of PalC to cortical sites even under acidic pH conditions (Hervás-Aguilar et al., 2010a). Moreover, ubiquitylated, rather than non-ubiquitylated *S. cerevisiae* Rim8p is preferentially recovered from Vps23 immunoprecipitates (Herrador et al., 2009), a finding also true for *A. nidulans* PalF (Fig. 7). However, in GST pull-downs, the *A. nidulans* Vps23 bait did not show any marked preference for PalF–Ub over PalF (Fig. 6). These results are consistent with the possibility that another Ub-binding module different from the Vps23 ubiquitin E2 variant (UEV), such as the carboxyl Npl4 zinc-finger (NZF) of Vps36 (Teo et al., 2006), contributes to a network of reinforcing interactions stabilising ESCRT proteins in cortical pH signalling complexes. Also not sufficiently understood is the fact that in contrast to *A. nidulans* PalF, whose ubiquitylation is strictly dependent on alkaline ambient pH and the 7-TMD receptor, Rim8p ubiquitylation is independent of both (Herrador et al., 2009), suggesting that Rim8p might be ubiquitylated through alternative inputs or receptors.

In *S. cerevisiae*, Vps23p binds to a SxP motif ($E^{533}SDP^{536}$) in Rim8p (Herrador et al., 2009) that resembles two Vps27p PSDP sequences containing a negatively charged residue that are recognised by a type-II-designated binding site in Vps23p (Ren and Hurley, 2011). This type II site is different from the type I binding site by which human Tsg101 (Vps23) binds P[S/T]AP motifs (Im et al., 2010). *A. nidulans* Vps23 lacks the basic binding pocket that accommodates the Asp residue in the Vps23p type II binding site (data not shown) (Ren and Hurley, 2011). In agreement, the equivalent of the $E^{533}SDP^{536}$ Rim8p SXP motif (Herrador et al., 2009) is PalF $A^{727}SAP^{730}$ (lacking the negatively charged residue). PalF has additional SXP motifs such as $P^{634}SQP^{637}$, $S^{700}SAP^{703}$, $P^{707}SRP^{710}$ and the 'type I-like' $P^{745}SAP^{748}$ that might be potentially recognised by *A. nidulans* Vps23. However, the physiological role(s) of these motifs (including $A^{727}SAP^{730}$) remains to be analysed.

An intriguing aspect of this model is the different roles that PalC and PalA, both direct Vps32 binders (Galindo et al., 2007; Rodríguez-Galán et al., 2009), play in plasma-membrane-associated signalling complexes. For both, recruitment to cortical sites is Vps32 dependent, but PalC acts upstream of PalA and precedes PalA in arrival at the complexes. These findings are consistent with the predicted 'late' role of PalA in pH signalling, as PalA is also able to bind PacC through two conserved YPx[L/I] motifs located either site of the signalling protease cleavage site in the transcription factor (Vincent et al., 2003). Thus, the current view is that PalA links PacC to

Vps32-containing complexes, 'presenting' the PacC substrate to the signalling protease PalB (Rim20p), itself an ESCRT-III interactor (Peñas et al., 2007; Rodríguez-Galán et al., 2009; Xu and Mitchell, 2001). Our data strongly indicate that signalling necessitates the Vps32-dependent PalA recruitment to the plasma membrane [in agreement with the finding that endosomal association of the PalA orthologue Rim20p is not sufficient to promote pH signalling (Boysen et al., 2010)]. They are consistent with the model in Fig. 9 in which most if not all these 'late' reactions would take place within ESCRT-containing pH signalling complexes associated with the plasma membrane, rather than endosomes as previously suggested (Mitchell, 2008; Peñalva et al., 2008).

PalA (Rim20p) is closely related to Bro1p, the founding member of the Bro1 domain-containing proteins (Kim et al., 2005), but does not play any role in the multivesicular body (MVB) pathway. Conversely, Bro1p does not play any role in pH signalling (Xu et al., 2004). PalC is less closely related to Bro1p although it also shows considerable similarity to the Bro1 domain across its Bro1-like domain, including a patch of residues conserved with Bro1p in which substitutions impair Vps32 binding and pH signalling (Galindo et al., 2007). A notable aspect of the model in Fig. 9 is that ESCRTs can be recruited to the plasma membrane without being involved in a membrane scission event. Experiments with liposomes strongly implicated ESCRT-III as the executioner of membrane scission during the formation of ILVs (Wollert and Hurley, 2010). A recent report showed that the Bro1 domain has the ability to regulate the membrane scission activity of ESCRT-III by regulating its stability (Wemmer et al., 2011). Thus it is tempting to speculate that the roles of PalA and PalC are related to the need to regulate the organisation and/or stability of ESCRT polymers in pH signalling complexes in a manner that is not conducive to membrane scission.

Materials and Methods

A. nidulans

A. nidulans minimal (MM) and complete medium (MCA) were used. MM usually contained 1% glucose and 5 mM ammonium tartrate as the carbon and nitrogen source, respectively. C-terminally tagged PalC–GFP, PalA–GFP, PalA–mCherry and Vps23–GFP were encoded by gene-replaced alleles, following established procedures (Szewczyk et al., 2006; Yang et al., 2004). *vps4-1* and *vps4-ha3* are gene-replacement alleles driving expression of Vps4 and (HA)3-Vps4 under the control of the $niiA^{p}$ promoter, which is inducible by nitrate and repressible by ammonium (Hervás-Aguilar and Peñalva, 2010). Thus, where indicated 10 mM nitrate (inducing conditions for $niiA^{p}$) or 5 mM urea (non-repressing conditions for $niiA^{p}$) was used instead of ammonium as nitrogen source. Watch minimal medium (WMM), used for all microscopy experiments, is a modified version of MM (Hervás-Aguilar et al., 2010a). Genotypes of the strains used in this work are given in supplementary material Table S1. Primers are listed in supplementary material Table S2.

Microscopy and imaging techniques

Microscopy, image analysis and image manipulation was carried out essentially as previously detailed (Hervás-Aguilar et al., 2010a; Pantazopoulou and Peñalva, 2009; Pantazopoulou and Peñalva, 2011). We used a Nikon Eclipse epifluorescence microscope equipped with a 100× 1.40 NA plan-apochromat objective and an inverted Leica DMI6000B microscope with 63× 1.4 NA or 100× 1.4 NA plan-apochromat objectives and an incubation chamber coupled to the microscope stage. Images were acquired with a Hamamatsu ORCA ER digital camera driven by Metamorph software (Molecular Dynamics), using Semrock Brightline GFP-3035B and TXRED-4040B (mCherry) filter sets. Recruitment of fluorescent versions of PalA, PalC and Vps23 to cortical structures was monitored as described previously (Galindo et al., 2007; Hervás-Aguilar et al., 2010a). Cells were cultured overnight in WMM containing 0.1% glucose (w/v) as the carbon source and adjusted to acidic pH with 25 mM NaH_2PO_4 (pH 5.2–5.3) before being washed with and shifted to the same medium adjusted to acidic (5.2), neutral (7–7.2; with 12.5 mM NaH_2PO_4 plus 12.5 mM Na_2HPO_4) or alkaline (8.2–8.3; with 25 mM Na_2HPO_4) pH. Image acquisition was started immediately after the shift. For quantification, PalC–GFP-, PalA–GFP- or Vps23–GFP-containing punctate structures were counted in at least 25 germlings per strain and pH condition, and the resulting data were normalized to the germling length.

To study the order of PalA and PalC arrival at cortical structures, cells were cultured for 16 hours at 25℃ in eight-well uncoated chambers (Ibidi, Germany) containing pH ~5 WMM and shifted to pH 7 WMM before immediately starting acquisition of time-lapse sequences of the GFP and mCherry channels using a Leica DMI6000 microscope. Time resolution, determined by the exposure times (1 seconds for GFP, 1.2 seconds for mCherry) and automated filter exchange was 4.4 seconds. Sequences for single PalA–mCherry and PalC–GFP transient fluorescence bursts ($n=50$) were then 'isolated' as 1.65 µm square regions of interest (ROIs) containing the cortical fluorescence. The red and green channels in each movie were analysed to determine the background, which was used individually to threshold the series and reduce the area corresponding to each fluorescent structure to a 0.9 µm diameter circle. Average intensity values within these circles were calculated and subsequently considered relative to the maximal average value in any given sequence, which was set as 100%. Paired PalA–mCherry and PalC–GFP data were plotted versus time, setting the 'zero' time point to the frame immediately preceding the start of the PalA–mCherry burst. Means and standard errors were then calculated for 50 structures.

Contrast adjustment, movie construction, thresholding, and colour alignment were made using Metamorph (Molecular Dynamics). Images were converted to 8-bits before being transferred to CorelDraw for annotation.

GST pull-down assays

GST–Vps23, GST–$Vps23^{UEV}$(1–159) and GST–PalH(507–714) were expressed in *Escherichia coli* JM109-pRIL and purified as described previously (Abenza et al., 2010). Strains expressing PalF–HA_3 or PalF–HA_3::Ub^{K48R} (Hervás-Aguilar et al., 2010a) were cultured overnight in acidic *Aspergillus* fermentation medium (MFA) medium (final pH 5.1–5.4) or, for alkaline pH shifts, cultured for 16 hours in pH ~4.3 MFA medium before transferring mycelia to pH ~8.3 MFA medium for 10 minutes (Hervás-Aguilar et al., 2007). Protein extracts were prepared from lyophilized mycelia as described previously (Abenza et al., 2010). Powdered mycelia were resuspended and lysed in binding buffer (BB): 20 mM Tris-HCl pH 8, 110 mM KCl, 5 mM $MgCl_2$, 1 mM dithiothreitol (DTT), 10% glycerol, 0.1% Triton X-100 2.5 µM Pefabloc, 2 µM pepstatin, 1.2 µM leupeptin, 5 µM MG132 and 5 mM *N*-ethylmaleimide. ~5 µl glutathione–Sepharose beads containing ~50 µg of bait proteins (GST–$Vps23^{UEV}$, GST–PalH(507–714) or GST–Vps23 were mixed with 1 mg of *A. nidulans* protein extract in 0.8 ml of BB, using Handee-Spin Columns (Pierce). The mix was rotated for 2 hours at 4℃ before collecting the beads, which were washed three times with 20 mM Tris-HCl pH 8, 175 mM KCl, 5 mM $MgCl_2$, 1 mM DTT and 0.1% Triton X-100, with a 15 minute rotation at 4℃ between the second and third washes. Bound proteins were eluted with SDS-PAGE loading buffer. Aliquots (1/5) were run in 7% (29:1 acrylamide:bis-acrylamide) SDS–PAGE gels that were blotted using anti-HA antibody as reported (Hervás-Aguilar et al., 2010a). Separate aliquots were run in parallel for Coomassie staining.

Immunoprecipitation

Cell extracts [2 mg protein in IP buffer (25 mM Tris-HCl, pH 7.2, 150 mM KCl, 5 mM $MgCl_2$, 1 mM DTT, 0.1% Triton X-100, 10% glycerol, 10 mM Pefabloc, 5 µM pepstatin, 5 µM leupeptin, 5 µM MG-132, 15 mM NEM and 1× EDTA-free Roche's inhibitor cocktail)] were incubated with 1.2 µg of mouse anti-GFP cocktail of monoclonal antibodies (Roche) for 3 hours at 4℃, before being mixed with Pierce Protein G plus agarose (12 µl per sample) and incubated for an additional 2 hours. Beads containing the immunocomplexes were recovered by centrifugation at 1000 ***g*** and washed with IP buffer before eluting bound materials with Laemmli loading buffer prior to their analysis by western blotting. Anti-GFP western blots were as described previously (Galindo et al., 2007).

Anti-Vps4 antiserum

Plasmid p1672 (pQEzzHis::Vps4) drives expression in *E. coli* of a fusion protein containing two tandem copies of the protein A 'Z' domain fused to the N-terminus of *A. nidulans* Vps4. A 30,000 ***g*** supernatant obtained from a lysate from overexpressing bacteria was mixed with 0.4 ml IgG–Sepharose and purified following recommendations of the supplier (GE Healthcare). The fusion protein (~2.5 mg) was used to immunise rabbits (Davids Biotechnology, Regensburg, Germany). This antiserum was used at 1/5000 in western blots, after blocking non-specific binding sites with 3% (w/v) skimmed milk and 0.03% (w/v) of *A. nidulans* mycelial powder. Peroxidase-coupled anti-rabbit IgG (GE Healthcare) was used as the secondary antibody (1:3000). The specificity of the antibody was demonstrated by the fact that the band corresponding to Vps4 was shifted to a position of lesser mobility after (HA)3 tagging.

PacC processing assays in Vps4-deficient cells

Cells were cultured in 50 ml MM containing 10 mM $(NH_4)_2SO_4$, 5 mM urea or 10 mM $NaNO_3$, as required, adjusted to pH 4.4 with 50 mM sodium citrate buffer,

pH 3.5. After a 15-hour incubation at 30°C, mycelia were collected by filtration (cellulose membranes, 0.45 µm, 47 mm diameter) and transferred to medium buffered to pH 8.5 with HEPES–NaOH, containing the same nitrogen sources. Mycelial samples were taken before and at different times after the pH shift, pressed dry, quick-frozen, lyophilised and processed for PacC western blot analysis (Hervás-Aguilar and Peñalva, 2010).

Database entries

The genes and proteins used in this work can be found in the Aspergillus genome database (AspGD, http://www.aspergillusgenome.org/) under the following database entry numbers: PalA, AN4351; PalB, AN0256; PalC, AN7560; PalH, AN6886; PalF, AN1844; Vps32, AN4240; Vps23, AN2521; Vps27, AN2701; Vps4, AN3061.

Acknowledgements

We thank Elena Reoyo for technical assistance.

Funding

This work was supported by Ministerio de Ciencia [grant number BIO2009-7281 to M.A.P.]; Comunidad de Madrid [grant number SAL/0246/2006 to M.A.P.]; the Biotechnology and Biological Sciences Research Council [grant numbers BB/D521781/1, BB/F01189X/1 to H.N.A. and, for the latter, Elaine Bignell]; and the Wellcome Trust [grant numbers 067878, 084660/Z/08/Z to H.N.A. and Joan Tilburn]. Deposited in PMC for immediate release.

Supplementary material available online at
http://jcs.biologists.org/lookup/suppl/doi:10.1242/jcs.098897/-/DC1

References

Abenza, J. F., Galindo, A., Pantazopoulou, A., Gil, C., de los Ríos, V. and Peñalva, M. A. (2010). *Aspergillus* RabB^{Rab5} integrates acquisition of degradative identity with the long-distance movement of early endosomes. *Mol. Biol. Cell* **21**, 2756-2769.

Araujo-Bazán, L., Peñalva, M. A. and Espeso, E. A. (2008). Preferential localization of the endocytic internalization machinery to hyphal tips underlies polarization of the actin cytoskeleton in *Aspergillus nidulans*. *Mol. Microbiol.* **67**, 891-905.

Boysen, J. H., Subramanian, S. and Mitchell, A. P. (2010). Intervention of Bro1 in pH-responsive Rim20 localization in *Saccharomyces cerevisiae*. *Eukaryot. Cell* **9**, 532-538.

Calcagno-Pizarelli, A. M., Negrete-Urtasun, S., Denison, S. H., Rudnicka, J. D., Bussink, H.-J., Munera-Huertas, T., Stanton, L., Hervás-Aguilar, A., Espeso, E. A., Tilburn, J. et al. (2007). Establishment of the ambient pH signaling complex in *Aspergillus nidulans*: PalI assists plasma membrane localization of PalH. *Eukaryot. Cell* **6**, 2365-2375.

Calcagno-Pizarelli, A. M., Hervás-Aguilar, A., Galindo, A., Abenza, J. F., Peñalva, M. A. and Arst, H. N., Jr (2011). Rescue of *Aspergillus nidulans* severely debilitating null mutations in ESCRT-0, I, II and III genes by inactivation of a salt tolerance pathway allows examination of ESCRT gene roles in pH signalling. *J. Cell Sci.* **124**, 4064-4076.

Díez, E., Álvaro, J., Espeso, E. A., Rainbow, L., Suárez, T., Tilburn, J., Arst, H. N., Jr and Peñalva, M. A. (2002). Activation of the *Aspergillus* PacC zinc-finger transcription factor requires two proteolytic steps. *EMBO J.* **21**, 1350-1359.

Espeso, E. A., Roncal, T., Díez, E., Rainbow, L., Bignell, E., Álvaro, J., Suárez, T., Denison, S. H., Tilburn, J., Arst, H. N. Jr et al. (2000). On how a transcription factor can avoid its proteolytic activation in the absence of signal transduction. *EMBO J.* **19**, 719-728.

Galindo, A., Hervás-Aguilar, A., Rodríguez-Galán, O., Vincent, O., Arst, H. N., Jr, Tilburn, J. and Peñalva, M. A. (2007). PalC, one of two Bro1 domain proteins in the fungal pH signalling pathway, localizes to cortical structures and binds Vps32. *Traffic* **8**, 1346-1364.

Herrador, A., Herranz, S., Lara, D. and Vincent, O. (2009). Recruitment of the ESCRT machinery to a putative seven-transmembrane-domain receptor is mediated by an arrestin-related protein. *Mol. Cell. Biol.* **30**, 897-907.

Herranz, S., Rodríguez, J. M., Bussink, H. J., Sánchez-Ferrero, J. C., Arst, H. N., Jr, Peñalva, M. A. and Vincent, O. (2005). Arrestin-related proteins mediate pH signaling in fungi. *Proc. Natl. Acad. Sci. USA* **102**, 12141-12146.

Hervás-Aguilar, A. and Peñalva, M. A. (2010). Endocytic machinery protein SlaB is dispensable for polarity establishment but necessary for polarity maintenance in hyphal tip cells of *Aspergillus nidulans*. *Eukaryot. Cell* **9**, 1504-1518.

Hervás-Aguilar, A., Rodríguez, J. M., Tilburn, J., Arst, H. N., Jr and Peñalva, M. A. (2007). Evidence for the direct involvement of the proteasome in the proteolytic processing of the *Aspergillus nidulans* zinc finger transcription factor PacC. *J. Biol. Chem.* **282**, 34735-34747.

Hervás-Aguilar, A., Galindo, A. and Peñalva, M. A. (2010a). Receptor-independent ambient pH signaling by ubiquitin attachment to fungal arrestin-like PalF. *J. Biol. Chem.* **285**, 18095-18102.

Hervás-Aguilar, A., Rodríguez-Galán, O., Galindo, A., Abenza, J. F., Arst, H. N., Jr and Peñalva, M. A. (2010b). Characterization of *Aspergillus nidulans* DidB^{Did2}, a non-essential component of the multivesicular body pathway. *Fungal Genet. Biol.* **47**, 636-646.

Hurley, J. H. and Hanson, P. I. (2010). Membrane budding and scission by the ESCRT machinery: it's all in the neck. *Nat. Rev. Mol. Cell Biol.* **11**, 556-566.

Im, Y. J., Kuo, L., Ren, X., Burgos, P. V., Zhao, X. Z., Liu, F., Burke, T. R., Jr, Bonifacino, J. S., Freed, E. O. and Hurley, J. H. (2010). Chrystallographic and functional analysis of the ESCRT-I/HIV-1 Gag PTAP interaction. *Structure* **18**, 1536-1547.

Ito, T., Chiba, T., Ozawa, R., Yoshida, M., Hattori, M. and Sakaki, Y. (2001). A comprehensive two-hybrid analysis to explore the yeast protein interactome. *Proc. Natl. Acad. Sci. USA* **98**, 4569-4574.

Kim, J., Sitaraman, S., Hierro, A., Beach, B. M., Odorizzi, G. and Hurley, J. H. (2005). Structural basis for endosomal targeting by the Bro1 domain. *Dev. Cell* **8**, 937-947.

Lefkowitz, R. J. and Shenoy, S. K. (2005). Transduction of receptor signals by β-arrestins. *Science* **308**, 512-517.

Mitchell, A. P. (2008). A VAST staging area for regulatory proteins. *Proc. Natl. Acad. Sci. USA* **105**, 7111-7112.

Nickerson, D. P., West, M. and Odorizzi, G. (2006). Did2 coordinates Vps4-mediated dissociation of ESCRT-III from endosomes. *J. Cell Biol.* **175**, 715-720.

Orejas, M., Espeso, E. A., Tilburn, J., Sarkar, S., Arst, H. N., Jr and Peñalva, M. A. (1995). Activation of the *Aspergillus* PacC transcription factor in response to alkaline ambient pH requires proteolysis of the carboxy-terminal moiety. *Genes Dev.* **9**, 1622-1632.

Osako, Y., Maemoto, Y., Tanaka, R., Suzuki, H., Shibata, H. and Maki, M. (2010). Autolytic activity of human calpain 7 is enhanced by ESCRT-III-related protein IST1 through MIT-MIM interaction. *FEBS J.* **277**, 4412-4426.

Pantazopoulou, A. and Peñalva, M. A. (2009). Organization and dynamics of the *Aspergillus nidulans* Golgi during apical extension and mitosis. *Mol. Biol. Cell* **20**, 4335-4347.

Pantazopoulou, A. and Peñalva, M. A. (2011). Characterization of *Aspergillus nidulans* RabC/Rab6. *Traffic* **12**, 386-406.

Peñalva, M. A. and Arst, H. N., Jr. (2004). Recent advances in the characterization of ambient pH regulation of gene expression in filamentous fungi and yeasts. *Annu. Rev. Microbiol.* **58**, 425-451.

Peñalva, M. A., Tilburn, J., Bignell, E. and Arst, H. N., Jr. (2008). Ambient pH gene regulation in fungi: making connections. *Trends Microbiol.* **16**, 291-300.

Peñas, M. M., Hervás-Aguilar, A., Múnera-Huertas, T., Reoyo, E., Peñalva, M. A., Arst, H. N., Jr and Tilburn, J. (2007). Further characterization of the signaling proteolysis step in the *Aspergillus nidulans* pH signal transduction pathway. *Eukaryot. Cell* **6**, 960-970.

Ren, X. and Hurley, J. H. (2011). Structural basis for endosomal recruitment of ESCRT-I by ESCRT-0 in yeast. *EMBO J.* **13**, 2130-2139.

Rodríguez-Galán, O., Galindo, A., Hervás-Aguilar, A., Arst, H. N., Jr and Peñalva, M. A. (2009). Physiological involvement in pH signalling of Vps24-mediated recruitment of *Aspergillus* PalB cysteine protease to ESCRT-III. *J. Biol. Chem.* **284**, 4404-4412.

Su, W., Li, S., Oakley, B. R. and Xiang, X. (2004). Dual-color imaging of nuclear division and mitotic spindle elongation in live cells of *Aspergillus nidulans*. *Eukaryot. Cell* **3**, 553-556.

Szewczyk, E., Nayak, T., Oakley, C. E., Edgerton, H., Xiong, Y., Taheri-Talesh, N., Osmani, S. A. and Oakley, B. R. (2006). Fusion PCR and gene targeting in *Aspergillus nidulans*. *Nat. Protoc.* **1**, 3111-3120.

Teis, D., Saksena, S. and Emr, S. D. (2008). Ordered assembly of the ESCRT-III complex on endosomes is required to sequester cargo during MVB formation. *Dev. Cell* **15**, 578-589.

Teo, H., Gill, D. J., Sun, J., Perisic, O., Veprintsev, D. B., Vallis, Y., Emr, S. D. and Williams, R. L. (2006). ESCRT-I core and ESCRT-II GLUE domain structures reveal role for GLUE in linking to ESCRT-I and membranes. *Cell* **125**, 99-111.

Vincent, O., Rainbow, L., Tilburn, J., Arst, H. N., Jr and Peñalva, M. A. (2003). YPXL/I is a protein interaction motif recognised by *Aspergillus* PalA and its human homologue AIP1/Alix. *Mol. Cell. Biol.* **23**, 1647-1655.

Wemmer, M., Azmi, I., West, M., Davies, B., Katzmann, D. and Odorizzi, G. (2011). Bro1 binding to Snf7 regulates ESCRT-III membrane scission activity in yeast. *J. Cell Biol.* **192**, 295-306.

Wollert, T. and Hurley, J. H. (2010). Molecular mechanism of multivesicular body biogenesis by ESCRT complexes. *Nature* **464**, 864-869.

Xu, W. and Mitchell, A. P. (2001). Yeast PalA/AIP1/Alix homolog Rim20p associates with a PEST-like region and is required for its proteolytic cleavage. *J. Bacteriol.* **183**, 6917-6923.

Xu, W., Smith, F. J., Jr, Subaran, R. and Mitchell, A. P. (2004). Multivesicular body-ESCRT components function in pH response regulation in *Saccharomyces cerevisiae* and *Candida albicans*. *Mol. Biol. Cell* **15**, 5528-5537.

Yang, L., Ukil, L., Osmani, A., Nahm, F., Davies, J., De Souza, C. P., Dou, X., Pérez-Balaguer, A. and Osmani, S. A. (2004). Rapid production of gene replacement constructs and generation of a green fluorescent protein-tagged centromeric marker in *Aspergillus nidulans*. *Eukaryot. Cell* **3**, 1359-1362.